Bio-optical variability associated with phytoplankton dynamics in the North Atlantic Ocean during spring and summer of 1991

M. Stramska and T. D. Dickey

Ocean Physics Group, Department of Geological Sciences, University of Southern California, Los Angeles

A. Plueddemann and R. Weller

Woods Hole Oceanographic Institution, Woods Hole, Massachusetts

C. Langdon and J. Marra

Lamont- Doherty Earth Observatory, Palisades, New York

Abstract. Bio-optical data recorded from April 30 to July 19, 1991, using a mooring located in the open ocean (59°35.6'N, 20°57.9'W) are described and interpreted. Five multi-variable moored systems (MVMS) were deployed in the upper 90 m to obtain concurrent, co-located measurements of horizontal currents, water temperature, photosynthetically available radiation (PAR), transmission of light at 660 nm (c_{660}), and stimulated chlorophyll fluorescence. In addition, meteorological and subsurface temperature data (12 depths from 80 to 310 m) were collected. When the mooring was deployed, surface waters were weakly stratified and there was little evidence of a phytoplankton bloom. Soon after the deployment, a marked increase in phytoplankton concentration occurred simultaneously with an increase of near-surface water temperature. The most striking observation was a period (year days 128-140) of strong mixed layer depth variability (daily amplitude of about 40 m) during which phytoplankton standing stock reached its maximum. During this period, phytoplankton biomass was mixed down to deeper waters at nighttime. As a result, the variability of the bio-optical parameters was extremely high, and deepwater phytoplankton concentration was much greater than would have been expected from the productivity estimates. Later, phytoplankton concentrations declined sharply in response to extremely stormy weather around year day 140. Once the storm passed (after day 143), surface waters stratified and the phytoplankton stock increased again, but the depth integrated biomass concentration did not reach as high values as before the storm. During this strong thermal stability period, fluorescence and c_{660} signals in near-surface waters were much higher than at depth, and displayed a diel cycle which was well correlated with PAR.

Introduction

Phytoplankton blooms in the North Atlantic have been investigated in the past by various means, including coarse resolution time series obtained from ocean weather station ships and continuous plankton recorders deployed from ships of opportunity [e.g., *Williams*, 1975; *Colebrook*, 1979]. Later, much attention was directed toward Coastal Zone Color Scanner (CZCS) data for the North Atlantic. These data revealed that the open ocean can sustain intense blooms over vast areas and extended time periods [*Esaias et al.*, 1986]. Recently, a few international research programs have been conducted to cover relatively large spans of time in the North Atlantic area [*Ducklow and Harris*, 1993]. Included among these efforts was the Marine Light - Mixed Layer (MLML) program which conducted field experiments in 1989 and 1991.

One of the important MLML strategies was to use moorings which allow sampling of physical and bio-optical variables at a fixed position in space, over time periods of several months, and with resolution of the order of minutes [*Dickey*, 1991; *Dickey et al.*, 1991, 1993, 1994]. Bio-optical variables can reveal abundances of phytoplankton, which play a key role for

optical variability in the open ocean [*Jerlov*, 1976; *Kirk*, 1983; *Morel and Prieur*, 1977; *Smith and Baker*, 1978]. For example, beam attenuation coefficient measurements at 660 nm are correlated with particle concentration [e.g., *Bartz et al.*, 1978; *Bishop*, 1986; *Bishop et al.*, 1986, 1992; *Spinrad et al.*, 1989; *Gardner et al.*, 1993], while stimulated fluorescence is correlated with chlorophyll concentration [e.g., *Smith and Baker*, 1986; *Bartz et al.*, 1988]. Thus, a mooring using such instrumentation is ideal for the examination of the physical/biological feedbacks within the mixed layer and the fate of phytoplankton populations.

An overview of the MLML mooring data collected in 1989 has been given in another paper [*Dickey et al.*, 1994] and more detailed aspects of the bio-optical variability have been discussed by Stramska and Dickey [1992b, 1993, 1994]. The present paper focuses on the fundamental time-depth variability of bio-optical parameters as recorded by the mooring instruments during the period of April 30 to July 19, 1991 (year days 120-200). The primary objectives of the paper are: (1) to quantify the temporal patterns of phytoplankton variability in the northeast Atlantic; (2) to identify and clarify the roles of various mechanisms that control the phytoplankton biomass in the water column, and particularly, to examine the progression of a spring bloom with the seasonal stratification of surface waters; (3) to form the basis of a framework for the interpretation of the biological and chemical processes investigated in shipboard surveys [e.g. *Langdon* et al., this

issue; *Marra et al.*, this issue]. The description of the bio-optical variability is complemented by an account of major physical events observed over the course of the experiment. Details concerning the physical variability may be found in the companion paper by Plueddemann *et al.* [this issue].

Methods

Our measurements were carried out from April 29 through September 6, 1991 (year days 120-249), in the North Atlantic (59°35.6'N and 20°57.9'W). Time series data described in this paper were obtained with multi variable moored systems (MVMS, [*Dickey et al.*, 1991]) and a surface meteorological system. Since some of the instruments experienced technical problems at the end of the deployment, we will limit the interpretation of the data to year days 120-200 (i.e., April 29-July 19).

The methodologies have been described before [*Dickey et al.*, 1991, 1993, 1994], and more details on our mooring design are included in the work by Plueddemann *et al.* [1993]. Thus only a short description is given here. The MVMS data presented below were collected with the following sensors: vector measuring current meters (VMCM, [*Weller and Davis*, 1980]), thermistors for water temperature measurements, photosynthetically available radiation (PAR) sensors with spherical collectors for measuring scalar irradiance within the visible spectral range [*Booth*, 1976], beam transmissometers (light wavelength of 660 nm, [*Bartz et al.*, 1978]), and in situ stimulated fluorescence sensors (blue excitation filter and red emission filter, [*Bartz et. al.*, 1988]). The MVMS systems sampled at nominal depths of 10, 30, 50, 70, and 90 m. In addition, water temperatures were measured at 80, 102, 118, 150, 166, 182, 198, 214, 230, 246, and 310 m using thermistors. Meteorological measurements on the surface buoy included wind speed and direction, barometric pressure, air and sea surface (2 m) temperatures, air humidity, and incident solar radiation (250-2500 nm). The basic sampling rate for the MVMS systems was either 1 min (at 10 and 50 m) or 128 s (at 30, 70, and 90 m). The meteorological and deepwater temperature data were acquired at 7.5-min intervals.

The fluorometric data were converted to chlorophyll concentrations (Chl *a*) using calibrations done before the mooring deployment (e.g., see *Marra and Langdon*, [1993] for details). It should be noted that the conversion from volts to Chl *a* in situ is affected by factors such as ambient light intensity [e.g. *Stramska and Dickey*, 1992a, b] and phytoplankton species composition. However, the calibration, even if not very exact, allows us to estimate Chl *a* biomass in the water and enables comparison of the output from different instruments. The data set was processed to produce 15 min, 8 hour, and daily averaged time series which were used for this study. Time series analyses were performed using the 15-min averaged data and applying algorithms described by *Bendat and Piersol* [1966]. The power spectra of the data sets were obtained using a Fourier transform of the covariance function, to which the Parzen weighting function was applied. The confidence limits for the coherence function were calculated following the method of *Bloomfield* [1976].

The primary productivity estimate shown in the next section was obtained by applying a "light-pigment" productivity model [*Kiefer and Mitchell*, 1983] to the mooring data. The phytoplankton dynamics were simulated by incorporating the Kiefer-Mitchell productivity model into a physical one-dimensional model of the turbulent mixed layer [*Mellor and Yamada*, 1982; *Blumberg and Mellor*, 1983], and by using mooring data to initialize and force the model. A detailed discussion of the model and numerical values of the parameters used for the calculations may be found in the work by *Stramska and Dickey* [1994].

Results

Physical Background

For detailed description of the meteorological and physical variability at the mooring site, see a companion paper by *Plueddemann et al.*, [this issue]. Here we will present only those physical data which are most relevant in the context of the interpretation of bio-optical data.

An overview of the meteorological conditions during the experiment is presented in Figure 1. We note that, depending on the cloudiness, the daily maximum incoming solar irradiance varied between 100 and 900 W m^{-2}. Winds were variable, and extremely high wind events corresponding to low barometric pressure systems were observed around days 140 and 162. Time series in Figure 1 also show the variability of the net heat flux. This flux was estimated using MLML meteorological data and bulk formulas [*Bunker*, 1976; *Large and Pond*, 1982; *Geernaert*, 1990; also see *Plueddemann et al.*, this issue]. Note, that the heat loss exceeded 200 W m^{-2} during some nights.

Time series of water temperature are plotted in the upper panel of Figure 2. The mixed layer depth (MLD), estimated as the depth at which the temperature change from the surface was 0.05° or 0.1°C, is shown in the bottom panel. This estimate was obtained using linear interpolation of the water temperature between instrument depths. These data indicate that at the beginning of the experiment (day 120), the water column was already somewhat stratified with a MLD of about 90 m (0.05°C criterion). Later, we observed a further increase of the surface water temperature with time, and as early as on day 121 the MLD decreased to about 10 m. The surface water warming was interrupted around day 127, during a period of high wind speed and increased heat loss from the ocean (see Figure 1). In response to these conditions, the MLD increased, and around day 140 it reached about 100 m due to very stormy weather. After day 143, near-surface water warming was apparent again, and by the end of June (year day 180), the surface water was about 5°C warmer than it was at the end of April (year day 120). Interestingly, this strong near surface stratification apparently prevented the significant thickening of the mixed layer (ML) during the storm which passed the mooring site around day 162. It is also interesting that in 1991 we never observed a mixed layer as deep as we had observed in 1989. For example, on year day 120 of 1989, the MLD was estimated to be ~500 m [*Dickey et al.*, 1994].

Based on the water temperature data, we define three characteristic time periods: (1) the first period is when surface waters were thermally stable and the ML shallow (year days 120-127), (2) the second period is when surface waters were weakly stratified and the ML deepened (year days 127-140), and (3) the third period is when thermal stratification increased and the ML shoaled again (after day 143). Later, we will describe in detail how biomass concentration within the mixed layer responded to these different thermal situations.

Daily averaged wind and current vectors are shown in Figure 3. Current speed during the experiment was usually less than 0.6 m s^{-1}, and even lower after day 160. There was no apparent
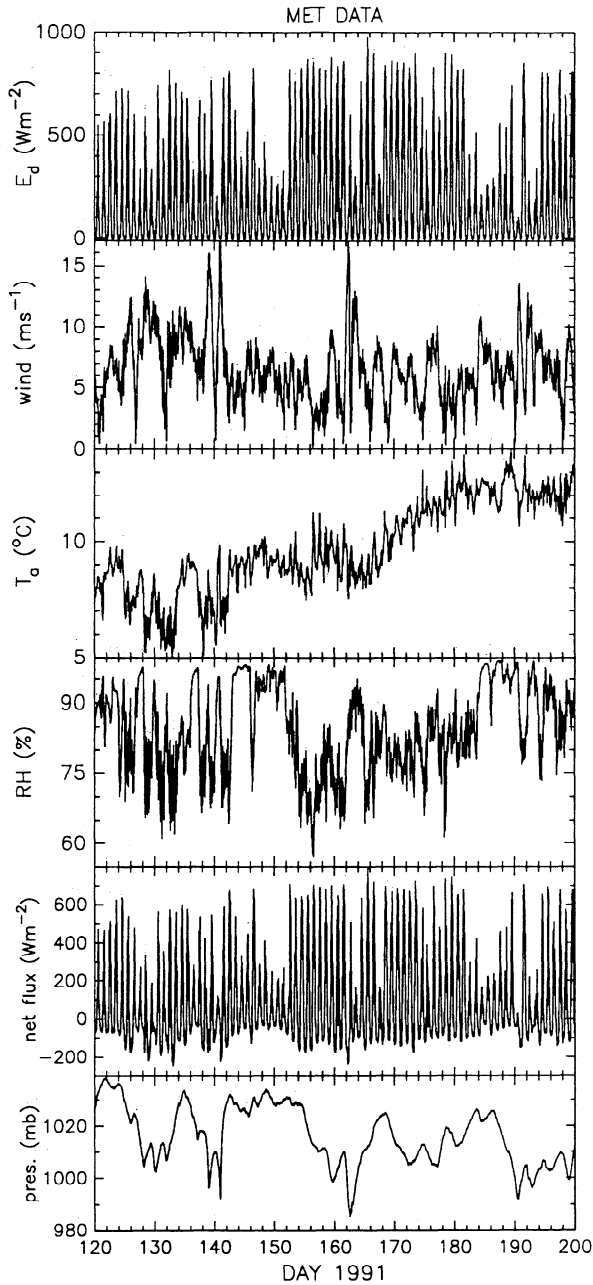
Figure 1. Time series of surface meteorological variables: downwelling irradiance (E_d), wind speed, air temperature (T_a), relative humidity (RH), net heat flux, and barometric pressure. These data were collected during the MLML 1991 experiment and are 15-min averages.

correlation in the direction of the local winds and currents, although an analysis similar to that described by *Dickey et al.* [1994] supports the notion that winds were important for the local near-surface shear (not shown here). Note that the most dramatic change in the current direction occurred on day 126, which corresponds to the beginning of the "deep ML" period. Later the direction of the current remained relatively constant.

Bio-Optical Observations

Time series of beam attenuation at 660 nm (c_{660}), chlorophyll *a* concentration from fluorometric measurements, and scalar irradiance (PAR) are shown in Figures 4, 5, and 6,
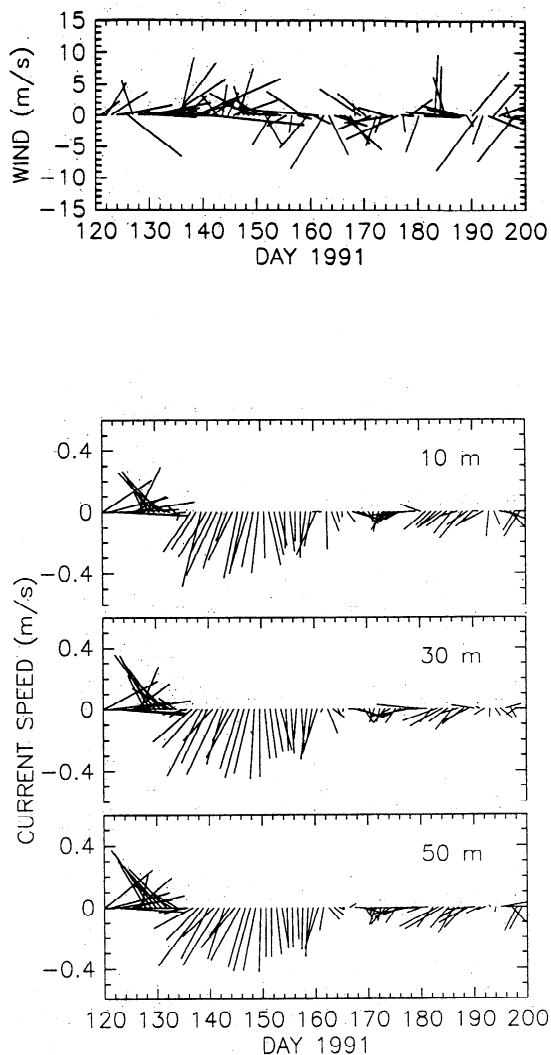
respectively. As seen in Figures 4 and 5, the initial increase in the water temperature was coincident with an increase in phytoplankton biomass. A strong bloom developed soon after the mooring was deployed, with the maximum Chl *a* concentration at 10-m depth exceeding 6 mg m^{-3}, and the maximum c_{660} was about 1 m^{-1}. Later we observed a relative minimum in the biomass concentration around day 140 corresponding to a storm system (see Figure 1). This was quickly followed by an increase of the biomass after day 143, as the waters stratified again. Note that these major features in biomass concentration variability are also reflected in the variability of the underwater PAR signal (Figure 6).

It is worthwhile to analyze in more detail the dependence of the biomass distribution in the water column on the mixed layer dynamics. The superimposed fluorescence time series at 10, 30, and 90 m are shown in the middle panel of Figure 7. The MLD is depicted in the bottom panel, where numbers 1, 2, and 3 denote the three time periods defined above. We note the following.

1.   When the ML was shallower (periods 1 and 3) the fluorescence and c_{660} signals were much higher in surface waters than at greater depths (see Figure 4 for c_{660}).

2.   When the ML was deeper (period 2), the bio-optical signals were high at all depths, even at 90 m. For example, Chl *a* concentration at 90-m depth, exceeded 4 mg m^{-3} and c_{660} was greater than 0.8 m^{-1}. As a result, the chlorophyll integrated over the 90-m water column was much higher during that period
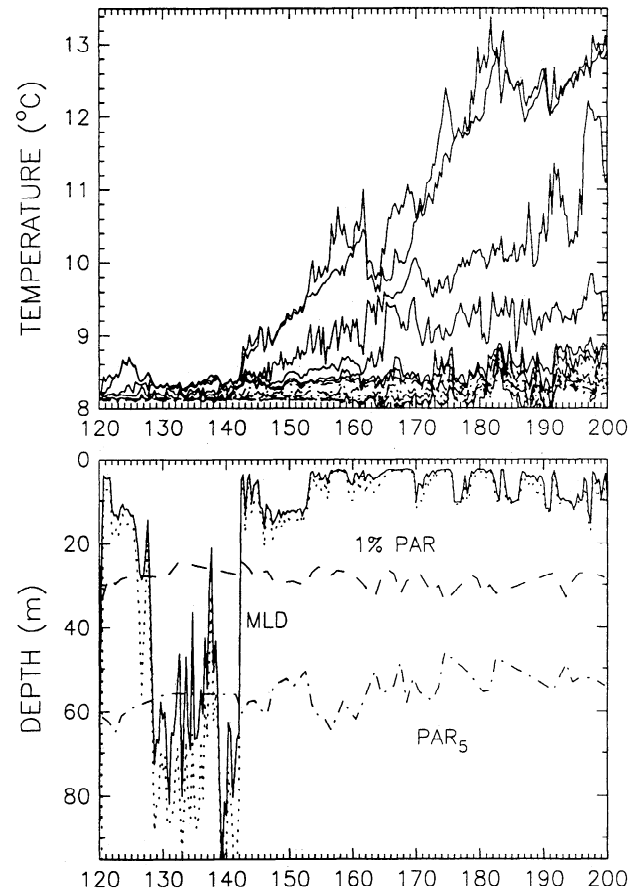
Figure 2. Time series of water temperature at 17 depths (2, 10, 30, 50, 70, 80, 90, 102, 118, 150, 166, 182, 198, 214, 230, 246, 310 m); 0.05°C (solid line) and 0.1°C (dotted) mixed layer depth; 1% and 5 mEinst m^{-2}s^{-1} (PAR 5) PAR level. Temperature data are 8-hour averages.

Figure 3. Time series of daily averaged wind and current vectors. North is directed up.

where E_{tot} is the total daily irradiance of PAR at the surface (Einst m^{-2} d^{-1}), K_{par} is the diffuse attenuation coefficient for PAR (m^{-1}), 0.8 is the correction term for surface reflectance and strong absorption of PAR at 650-700 nm in the surface waters, and E_c is the compensation intensity taken as 3.1 Einst m^{-2} d^{-1} [see *Langdon et al.*, this issue].

The term "critical depth", often used by biologists, was first defined by *Sverdrup* [1953] as the depth where vertically integrated, daily primary production is not smaller than the community losses by respiration. However, we would like to point out here that Sverdrup's classic model is a considerable simplification for our data set. This is because Sverdrup assumed a uniform mixing layer which was actively mixing at all times. Contrary to this assumption, our time series for "period 2" document strong variability of the surface water stability, which was changing significantly on the timescale of hours. Note also that the critical depth estimate depends strongly on the values of the parameters used for such computations [*Nelson and Smith*, 1991; *Smetacek and Passow*, 1990].

High biomass concentration in deep waters during "period 2" (Figure 8d) is not likely to be accounted for by local growth at these depths. Such a notion is supported by the time-depth

of time than during the other two periods (Figure 7, upper panel). At first glance it may even appear paradoxical, as our data suggest a relation opposite to what is commonly expected (i.e, we observed more intense phytoplankton bloom when the mixed layer was relatively deep). However, as we will see next, this temporal behavior of the phytoplankton stock can be viewed as a specific example of the balance between physical and biological processes.
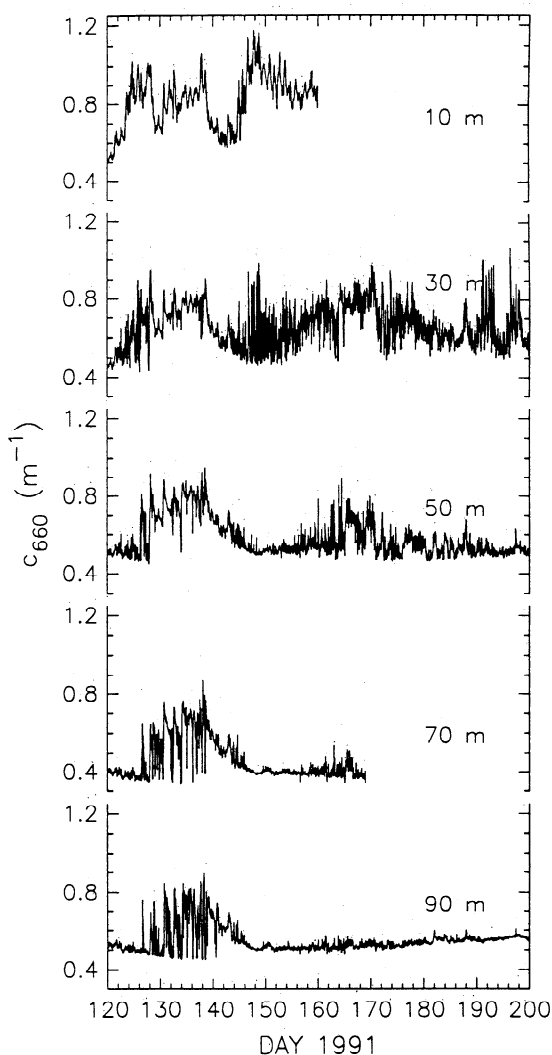
To explain this point and to illustrate that changes in biomass were closely coupled to physical conditions, two 10-day subsets of time series data were selected. These two examples are shown in Figures 8 and 9, corresponding to "deeper" and "shallower" mixed layer periods (periods 2 and 3 in Figure 7). The "deeper" ML period is actually characterized by large-amplitude fluctuations in the MLD (Figure 8a). Importantly, the ML was often shallow enough to allow intense phytoplankton growth in the near-surface water. Note that during that period of time the "critical depth" was very close to the MLD (Figure 7). Critical depth (Z_c) was estimated according to the formula given by *Nelson and Smith* [1991]:
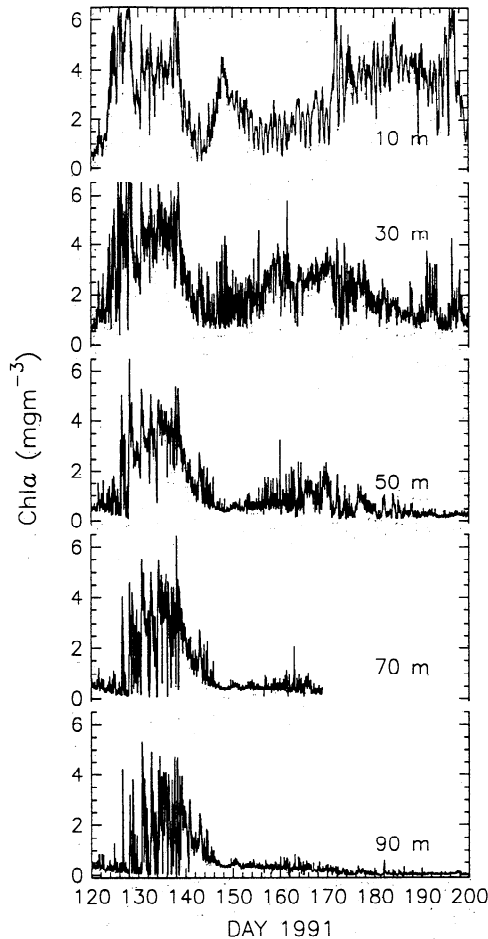
$$Z_c = 0.8 E_{tot}/(K_{par} E_c)$$

Figure 4. Time series of beam attenuation coefficient at 660 nm at 10-, 30-, 50-, 70-, and 90-m depths. Note that parts of the 10- and 70-m records are missing due to instrument failure.

Figure 5. Time series of fluorometrically determined concentrations of chlorophyll a at 10-, 30-, 50-, 70-, and 90-m depths. Part of the 70-m record is missing due to instrument failure.

primary production contour for the MLML experiment shown in Figure 10. This primary production estimate was obtained by applying the Kiefer-Mitchell productivity model [*Kiefer and Mitchell*, 1983] to the Chl *a* and PAR time series shown in Figures 5 and 6. According to the model calculations, primary production at the 50-m and greater depths was relatively low because of the low light intensity. Thus, we suggest that the observed high concentration of phytoplankton in deep waters must be explained by the fact that phytoplankton were effectively mixed down there, from near the surface. This conclusion is based also on the fact that the temporal variations in the temperature record closely resemble those in the fluorescence and c_{660} records. This can be seen in Figure 8 d, where sudden changes in the 50-m water temperature correspond to similar changes in bio-optical signals.

The visual recognition of a strong relationship between water temperature and bio-optical properties is supported by the results of spectral analysis. The coherence and phase functions estimated for the water temperature and c_{660} records at 10 m are shown in Figure 11 (middle panels). To a first approximation, one can interpret our problem as a single-input, single-output physical system, where water temperature is an input and bio-optical properties are the outputs. For the ideal case of a linear system, the coherence function would be unity. Our realistic system has the coherence less than unity, which can result from
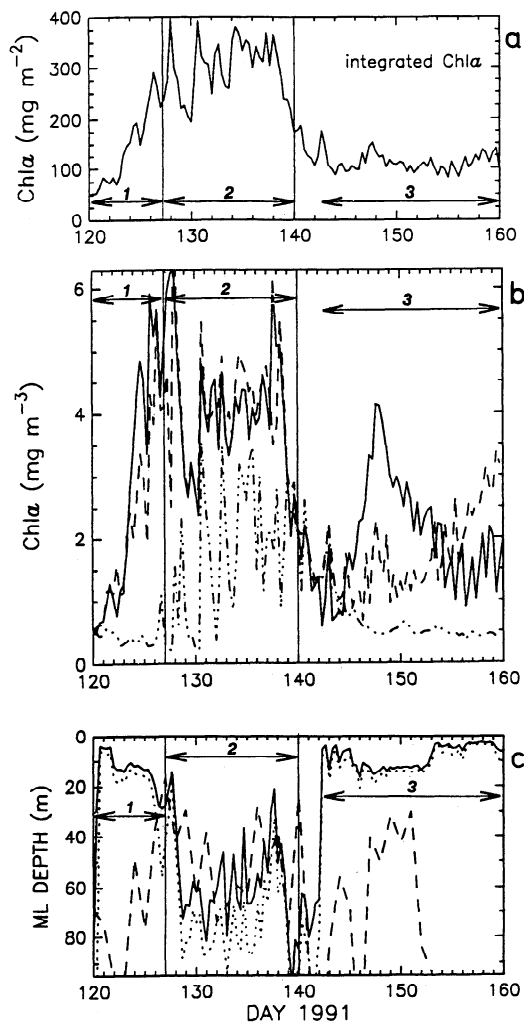
the nonlinear response or the presence of other inputs that contribute to the output signal (affect bio-optical variability).

It should be noted that, in general, the strong coherence between water temperature and bio-optical properties could arise from both vertical mixing and/or advection of different water masses. Although we cannot completely rule out the latter possibility without measurements taken simultaneously in time and providing some horizontal coverage, we note that there is no evidence for strong advection in the time series of local currents. Furthermore, changes of the water temperature at 10-m depth (Figure 8a) compared with local net heat flux (Figure 8b) indicate that a significant part of the temperature variability is likely to be of local origin. The results of the spectral analysis for the net heat flux and 10-m temperature are shown in Figure 11 (top panels). Highly significant coherence (about 0.75) was found between these two variables, which supports our conclusion.

The second 10-day subset of time series is shown in Figure 9 and represents the conditions of relatively strong thermal stratification of surface waters (days 149-159, which are in period 3, Figure 7). The data presented in Figure 9a indicate that the MLD was less than 20 m, due to intense heating and weak winds. The bio-optical signals (Figures 9c and 9d) show very different behaviors than during period 2 (Figures 8c and 8d). First, high fluorescence and c_{660} signals were restricted to surface waters and their magnitude decreased rapidly with depth.
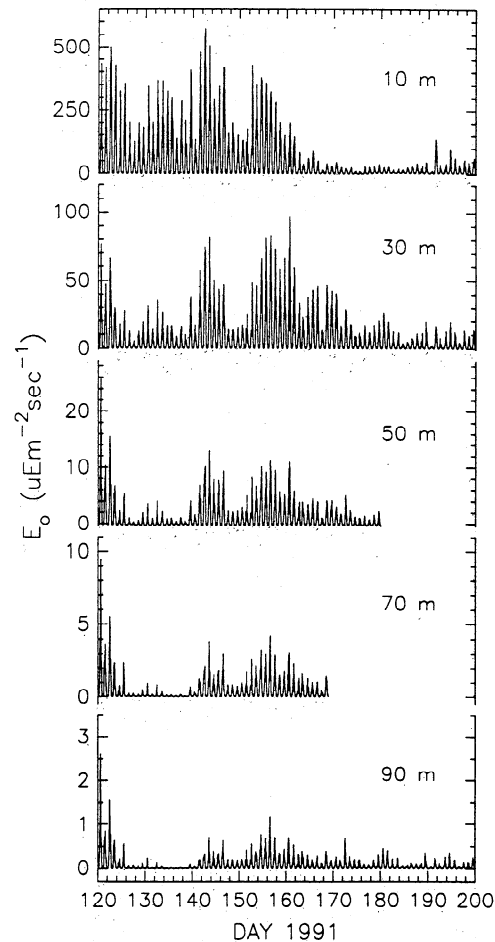
Figure 6. Time series of PAR at 10-, 30-, 50-, 70-, and 90-m depths. Parts of the 50- and 70-m records are missing due to instrument failure.
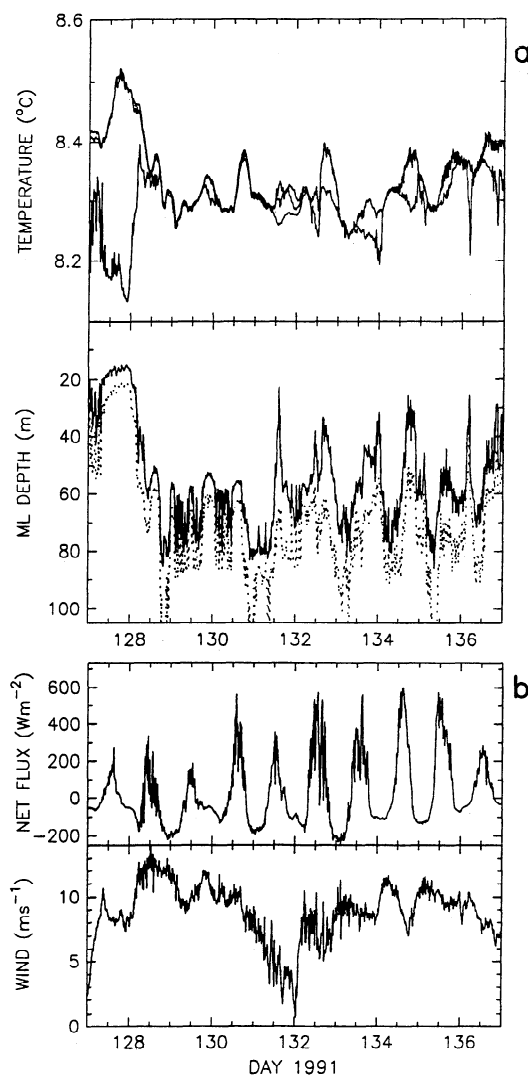
Discussion and Conclusions

Our MLML time series collected in 1989 and 1991 show that there is large inter-annual variability in the scenario of high-latitude North Atlantic spring blooms. For example, there were obvious differences in the timing of progress of the water's thermal stratification, with periods of extremely deep mixing observed only during the 1989 experiment. As a result, the bloom in 1991 apparently began a few weeks earlier than in 1989 (day 120 compared to day 140, see *Dickey et al.*, [1994] for the 1989 mooring data). Additionally, the Chl *a* concentration in the spring of 1991 was significantly higher than in 1989.

The most striking observation in the 1991 data set was the several day long period of strong MLD variability (with 0.05°C MLD daily amplitude of about 40 m) during which phytoplankton standing stock reached a maximum. During this period, phytoplankton biomass was mixed down to greater depths during nighttime. As a result, the variability of the bio-

Figure 7. (a) Time series of water column integrated phytoplankton biomass. This was calculated using the Chl a time series shown in Figure 5. (b) Superimposed time series of fluorometrically determined concentration of chlorophyll a at 10 (solid line), 30 (dashed line), and 90 m (triple dot-dash). (c) Time series of 0.05°C (solid line) and 0.1°C (dotted line) mixed layer depth, and "critical depth" (dashed line) estimated using formula given by Nelson and Smith [1991].

Second, it appears that deep waters were well isolated from above, because there was basically no correlation between the bio-optical signals at 10- and 50-m depths (the same was true for the water temperature at 10- and 50-m depths, Figure 12). Third, characteristic diel cycles in c_{660} and fluorescence were apparent at 10-m depth [e.g. *Stramska and Dickey*, 1992b], but there was no strong correlation between bio-optical parameters and water temperature at this depth. In contrast, at greater depths there was a strong correlation of bio-optical properties with water temperature, including intense short-term variability, which was probably related to the presence of internal waves [e.g., *Denman*, 1976]. All of these relationships, which are relatively easy to assess by a visual inspection of the data plotted in Figure 9, were supported by the spectral analysis. Only the most important results of the spectral analysis are summarized in Figure 12.

Figure 8. The 10-day subset of the MLML data from the period of extremely variable MLD. (a) Water temperature (at 2, 10, and 50 m), and mixed layer depth. (b) Meteorological data: net heat flux and wind speed. (c) 10-m data: PAR, chl a, c_{660}, and water temperature. (d) 50-m data: PAR, chl a, c_{660}, and water temperature.
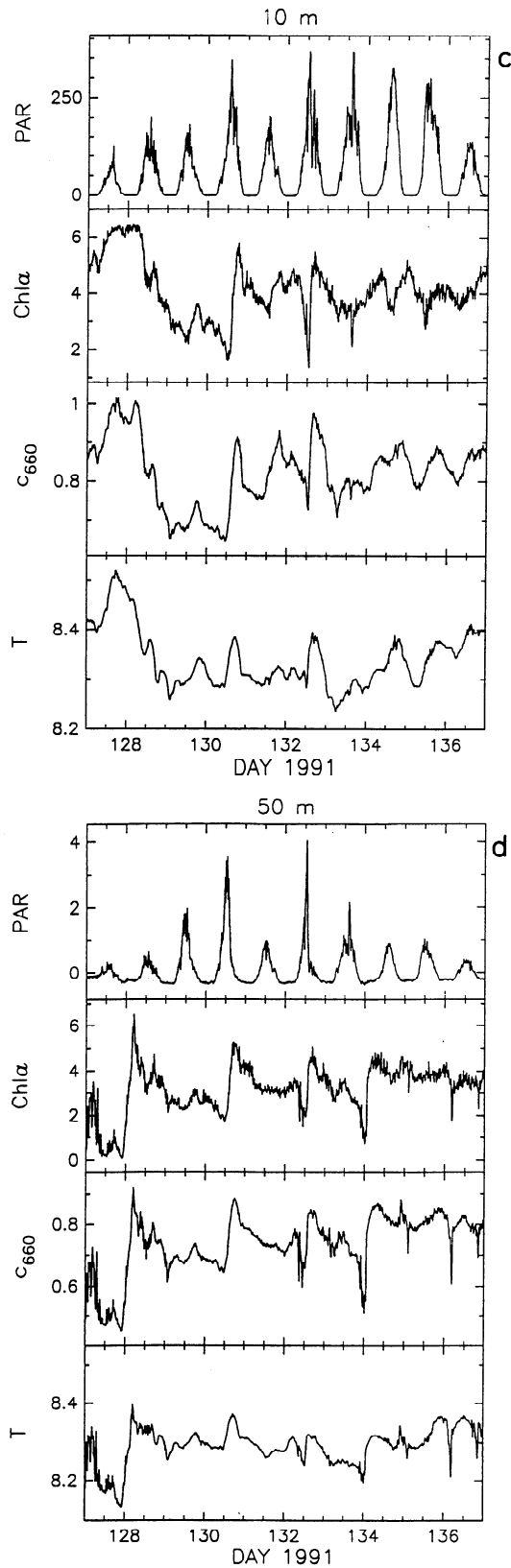
Figure 8. (continued)

time period of stable stratification, we observed strong blooming, but depth integrated phytoplankton biomass was lower than in "period 2". The fluorescence and c_{660} signals were much higher in surface waters than at depth, and characteristic diel cycles (in response to PAR variability) were present in fluorescence and c_{660} at 10-m depth. At greater depths, the variability in the bio-optical parameters was strong on a short timescale and correlated with water temperature.

It should be borne in mind, that during both observational periods (Figures 8 and 9) the surface water temperature displayed a daily cycle of variability. The theoretical description of such variability and its implications for mixed layer dynamics has been modeled by several authors [*Kondo et al.*, 1979; *Dickey and Simpson*, 1983; *Price et al.*, 1986; *Woods and Barkmann*, 1986]. According to the results of these models, turbulent mixing of the surface waters extends to shallower depths during the day than at night because solar heating inhibits the mixing associated with wind action. The precise amplitude of the daily thermocline depends on the weather, especially cloud cover and winds, which may enhance or decrease the changes related to seasonal variability. Note that the diel thermal cycle is of special importance for biological/physical feedbacks since this timescale coincides with the generation time of individual phytoplankters.
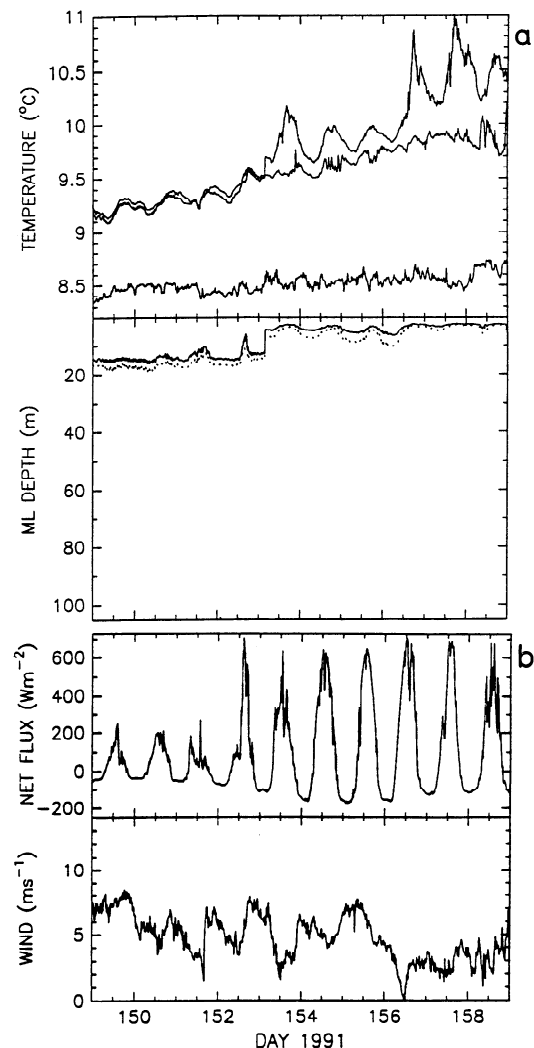

optical parameters was extremely high, and deepwater phytoplankton biomass was much higher than would have been expected from the primary productivity estimates. These conditions changed around day 143 when surface waters stratified and the 0.05°C MLD was less than 20 m. During the

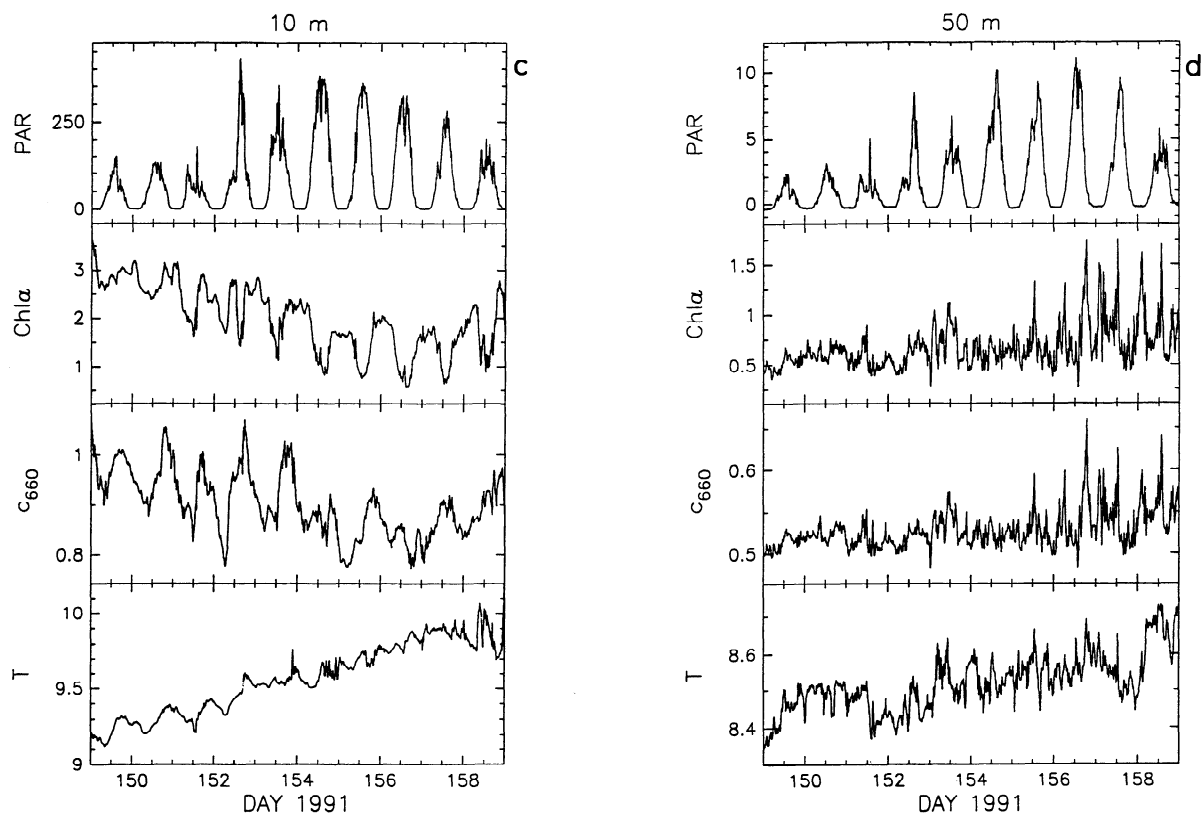**Figure 9.** Same as Figure 8, but for the period of little variability in MLD.

Figure 9. (continued)

It seems that our period 2 is a very energetic case of such a diel cycle in ML stratification. Indeed, the conditions at that time were characterized by considerable wind stirring and intense heat loss during nighttime, alternating with significant input of solar radiation during daytime, with low daily average heat flux ($\sim$20 W m^{-2}). The nighttime deepening of the mixed layer was reflected in deep penetration of the spring bloom.

Such intense mixing likely assured a good supply of nutrients, while the removal of the phytoplankton stock from the surface increased the transmission of solar energy over the next day. The reduction of mixing during the day was critical for the high growth rate; the phytoplankton production in the well-lighted surface waters during the day must have been sufficient to compensate for cells being transported down to greater depths
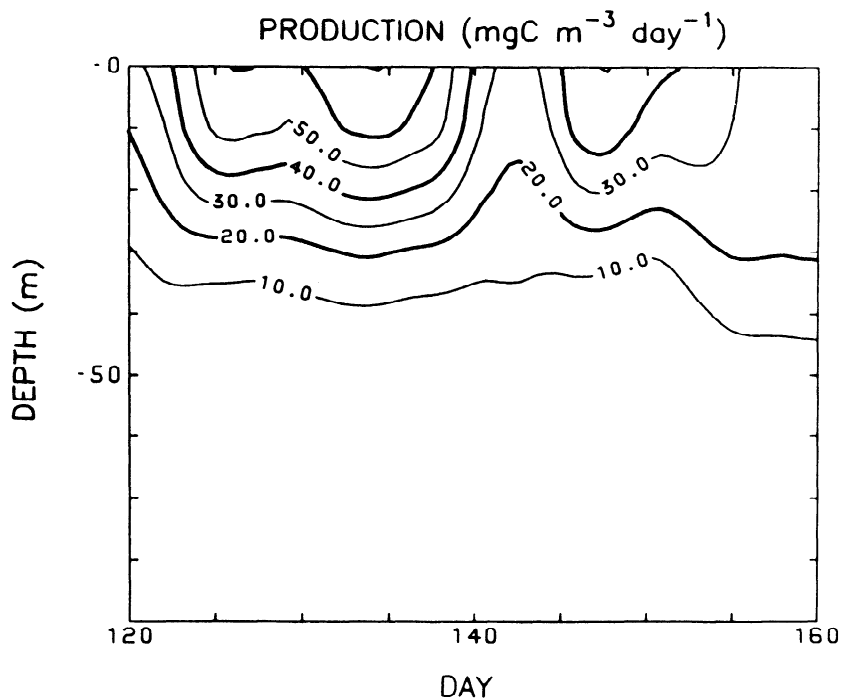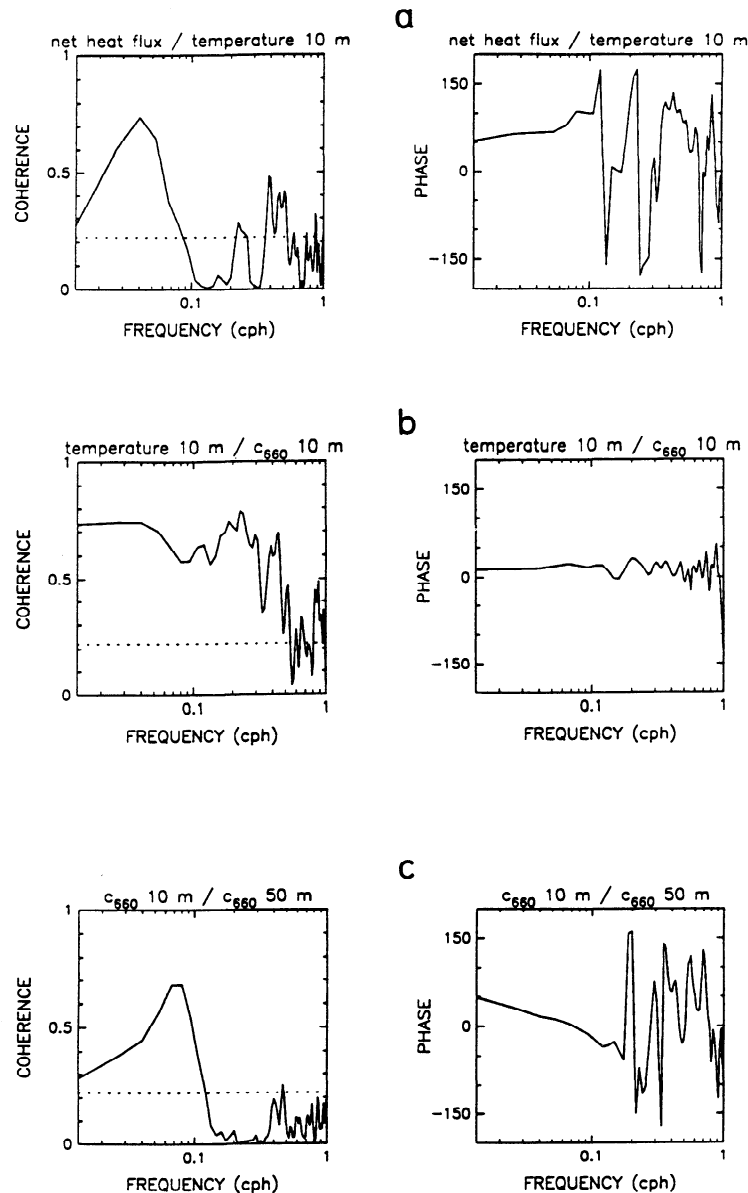

Figure 10. Primary production estimated from Chl a and PAR time series (shown in Figures 5 and 6), using the Kiefer and Mitchell [1983] model.
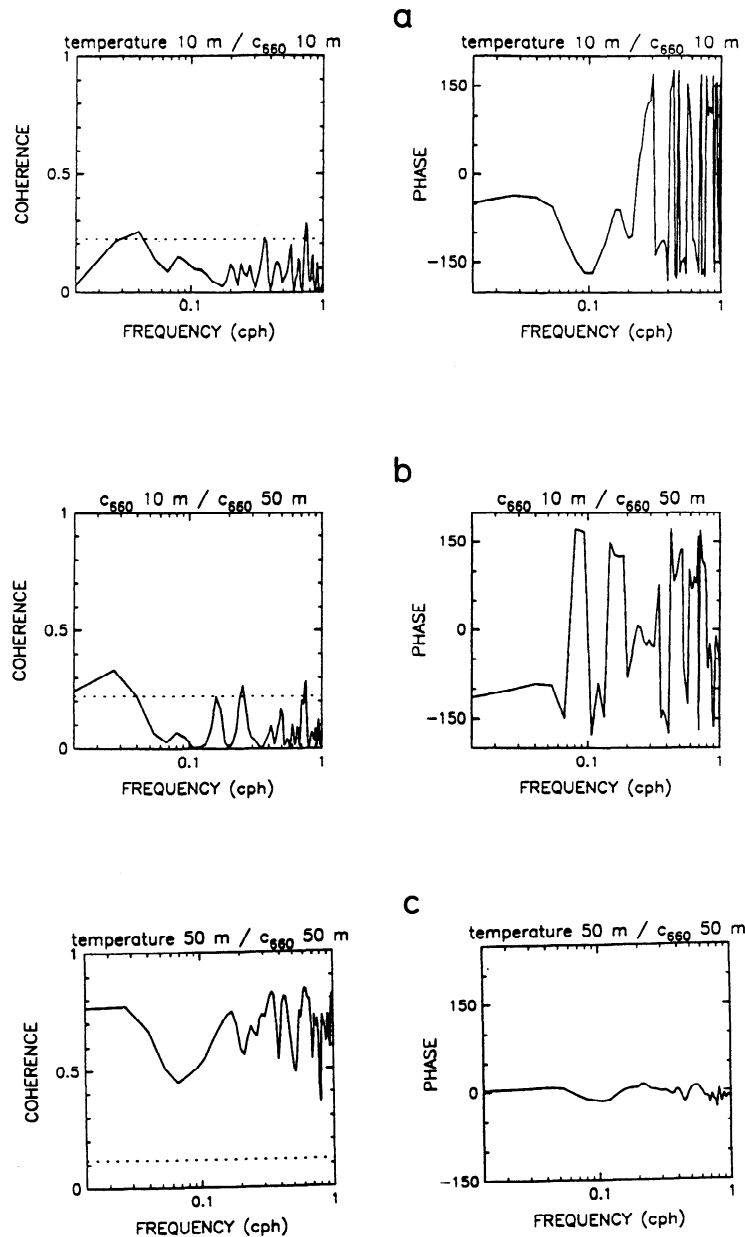
Figure 11. Squared coherence and phase function between (a) net heat flux and 10-m water temperature, (b) water temperature and c_{660} at 10-m depth, (c) c_{660} at 10- and 50-m depths. These are estimates for the 10-day subset of the MLML data shown in Figure 8. Dashed line is a 95% cutoff value.

during the night. The optimum conditions for high phytoplankton production also required that the overnight decrease of phytoplankton concentration in surface waters was not too large, because total production is proportional to the product of the growth rate and chlorophyll concentration.

We can view the above scenario as a special equilibrium between physical and biological conditions which lead to extremely favorable conditions for phytoplankton growth. Note, that the probability of occurrence of such a balanced situation may partially explain large inter-annual variation of phytoplankton biomass in the North Atlantic waters. In general, if the daily heating of the surface waters starts to prevail over the nighttime cooling, then the trend of increasing thermal stratification should be observed. This in turn must result in a separation of the surface and deep waters similar to this described for our period 3 (Figure 9). The "moderate" diel cycle associated with such a situation has been reproduced

before for data from the spring of 1989 by *Taylor and Stephens* [1993] and *Stramska and Dickey* [1994], although different modeling approaches were used. The important observation now is that the conditions of a "moderate" diel cycle lead to a somewhat smaller total biomass in the water column compared to the "intense thermal diel variability" period. On the other hand, if the overnight cooling is not compensated by the diurnal warming, then the deepening of the ML should be observed. This may lead to a significant dilution of the biomass in the water column which will not be replaced by a newly produced phytoplankton. An example of such conditions is the decrease of phytoplankton concentration in response to stormy weather around day 140 (Figure 7). Similar examples for the 1989 data are discussed by *Stramska and Dickey* [1994].

High coherence between net heat flux and 10-m water temperature (Figure 11) supports our interpretation of the data primarily in terms of the local variability. Importantly, we

Figure 12. Squared coherence and phase function between (a) water temperature and c_{660} at 10-m depth, (b) c_{660} at 10- and 50-m depths, (c) water temperature and c660 at 50-m depth. These are estimates for the 10-day subset of the MLML data shown in Figure 9. Dashed line is a 95% cutoff value.

were able to simulate a similar pattern of intense diel changes with a 1-D mixed layer model. A full description of the model and numerical values of the parameters used for the calculations are given by *Stramska and Dickey* [1994]. The model was forced with the boundary conditions estimated from the meteorological and mooring data on days 125-137. The temperature and Chl a time series from this model simulation are shown in Figure 13. The behavior of the model resembles that of the experimental time series, which plausibly suggests that the variability of the biomass concentration may be attributed in large part to local processes. The model estimate of the phytoplankton export out of the euphotic waters (taken here to be 50 m deep) is shown in the bottom panel of the Figure 13. This is presented as the ratio of the net Chl *a* flux out of the euphotic waters to the total production in the water column,

both integrated over a day. The results shown in Figure 13 indicate the great importance of the increased mixing for the removing of phytoplankton from the surface. Because of the simplicity of the biological part of the model and the lack of in situ measurements for the biological parameters, the quantitative interpretation of these results must be done with caution. However, because the model did not take into account cell sinking, it underestimated rather than overestimated total export of the biomass to deep waters.

What is the fate of the cells which were mixed to deeper waters? According to the interpretation of some previous modeling results [e.g., *Woods and Onken*, 1982; *Lande and Wood*, 1987], the phytoplankton that were mixed down by the nighttime convection may be separated from the mixed layer by the daily thermocline. Cells would accumulate in a deeper layer
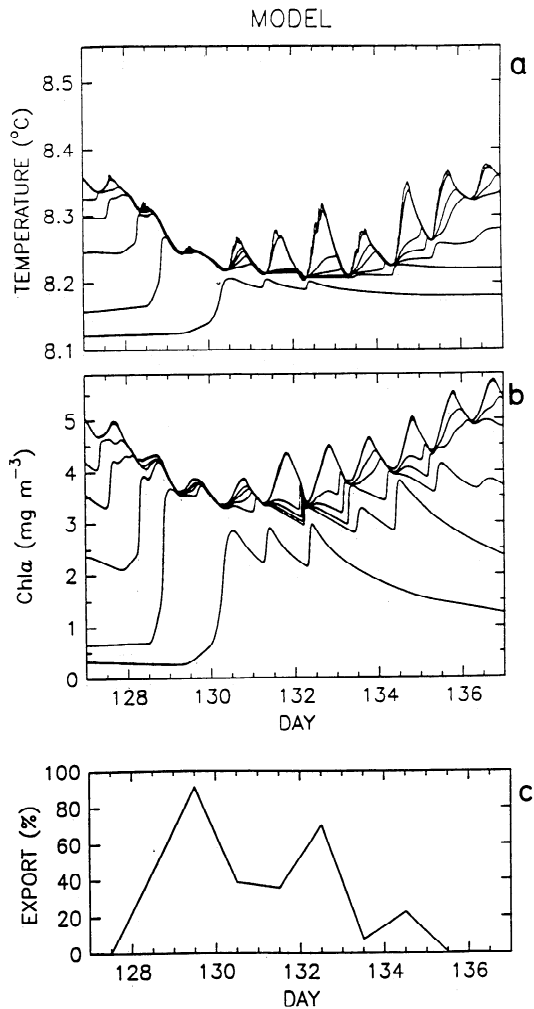
MODEL

Figure 13. (a) Modeled time series of water temperature. (b) Modeled time series of Chl a concentration. Curves are shown for 2, 11, 33, 41, 50, 60, 76 m. (c) Model estimate of the biomass export from the 50-m deep surface layer due to vertical mixing. It has been calculated as the ratio of the net turbulent flux of the Chl a at 50-m depth to the total production of Chl a in the water column, both integrated over a day.

and their depth would change very little with time due to low sinking rates. They would thus contribute to the deep phytoplankton maximum. It was further suggested that some of the cells may be reentrained by the next nighttime convection back into the mixed layer. It was also suggested that, in a similar way, spring storms may provide a mechanism for returning the phytoplankton to near the surface.

While this description of the phytoplankton fate may be appropriate in some circumstances (deep biomass maximum), the explanation for our observations seems different. We believe that intermittent mixing due to synoptic wind forcing and large-amplitude diurnal changes in mixed layer thickness in the spring acted to remove phytoplankton from surface waters. This is in agreement with the fact that both primary production and phytoplankton concentration were much higher in surface waters than at depth during our experiment. Thus the net flux of particles by vertical mixing had to be directed downward. Such an effect of the mixing on the particle removal has been suggested before [*Gardner et al.*, 1993; *Stramska and Dickey*, 1994]. Interestingly, after the fast increase of the biomass in

deep waters due to each mixing event, our data show slow but persistent decreases in the Chl a and c_{660} with time. If a quiescent flow is assumed in deep waters, then such a decrease of biomass cannot be explained only by the low cell sinking rates. In the actual ocean, the dispersion of particles is probably more efficient because of the role of processes not included in the model. These may include mixing induced by internal wave breaking and oceanic fronts, or aggregate formation [e.g., *Holligan et al.*, 1985; *Hill*, 1992].

Finally, if our interpretation is correct, then the bio-optical properties in the open ocean may be highly variable on relatively short time scales due to local dynamical processes (twofold changes within a few hours at 10-m depth). This variability is a consequence of the critical dependence of biomass on mixing. Large errors in the interpretation of the data may be induced if physical conditions are not well known, or if the data collected in the sea have inadequate temporal resolution [*Wiggert et al.*, 1994].

References

Bartz, R., J. R. V. Zaneveld, and H. Pak, A transmissometer for profiling and moored observations in water, Ocean Optics 5, *Proc. SPIE Int. Soc. Opt. Eng.*, *160*, 102-108, 1978.

Bartz, R., R. Spinrad, and J. C. Kitchen, A low power, high resolution, *in situ* fluorometer for profiling and moored applications in water, Ocean Optics 9, *Proc. SPIE Int. Soc. Opt. Eng.*, *925* 157-170, 1988.

Bendat, J. S., and A. G. Piersol, *Measurement and Analysis of Random Data*, 390 pp., John Wiley, New York, 1966.

Bishop, J. K. B., The correction and suspended particulate matter calibration of Sea Tech transmissometer data, *Deep Sea Res.*, *33*, 121-134, 1986.

Bishop, J. K. B., M. H. Conte, P. H. Wiebe, M. R. Roman, and C. Langdon, Particulate matter production and consumption in deep mixed layers: Observation in a warm-core ring, *Deep Sea Res.*, *33*, 1813-1841, 1986.

Bishop, J. K. B., R. C. Smith, and K. S. Baker, Springtime distribution and variability of biogenic particulate matter in Gulf Stream warm-core ring 82B and surrounding N.W. Atlantic waters, *DeepSea Res.*, *39*, suppl.#1A, S295-S325, 1992.

Bloomfield, P., *Fourier Analysis of Time Series: An Introduction*, 258 pp., John Wiley, New York, 1976.

Blumberg, A. F., and G. L. Mellor, Diagnostic and prognostic circulation studies of the South Atlantic Bight. *J. Geophys. Res.*, *88*, 4579-4592, 1983.

Booth, C. R., The design and evaluation of a measurement system for photosynthetically active quantum scalar irradiance, *Limnol. Oceanogr.*, *19*, 326-335, 1976.

Bunker, A. F., Computations of surface energy flux and annual air-sea interaction cycles of the North Atlantic Ocean, *Mon. Weather Rev.*, *104*, 1122-1140, 1976.

Colebrook, J. M., Continuous plankton records: Seasonal cycles of phytoplankton and copepods in the North Atlantic Ocean and the North Sea, *Mar. Biol.*, *51*, 23-32, 1979.

Denman, K. L., Covariability of chlorophyll and temperature in the sea, *Deep Sea Res.*, *23*, 539-550, 1976.

Dickey, T. D., The emergence of concurrent high resolution physical and bio-optical measurements in the upper ocean and their applications, *Rev. Geophys.*, *29*, 383-413, 1991.

Dickey, T. D., and J. J. Simpson, The influence of optical water type on the diurnal response of the upper ocean, *Tellus*, *35B*, 142-154, 1983.

Dickey, T. D., J. Marra, T. Granata, C. Langdon, M. Hamilton, J.

Wiggert, D. Siegel, and A. Bratkovich, Concurrent high resolution bio-optical and physical time series observation in the Sargasso Sea during the spring of 1987, *J. Geophys. Res.*, *96*, 8643-8664, 1991.

Dickey, T. D., T. Granata, J. Marra, C. Langdon, J. Wiggert, Z. Chai-Jochner, M. Hamilton, J. Vazquez, M. Stramska, R. Bidigare and D. Siegel, Seasonal variability of bio-optical and physical properties in the Sargasso Sea, *J. Geophys. Res.*, *98*, 865-898, 1993.

Dickey, T. D., J. Marra, M. Stramska, C. Langdon, T. Granata, R. Weller, A. Plueddemann, and J. Yoder, Bio-optical and physical variability in the sub-arctic North Atlantic ocean during the spring of 1989, *J. Geophys. Res.*, *99*, 22,541-22,556, 1994.

Ducklow, H. W., and R. P. Harris, Introduction to the JGOFS North Atlantic Bloom Experiment, *Deep Sea Res.*, *40*, 1-8, 1993.

Esaias, W. E., G. C. Feldman, C. R. McClain, and J. A. Elrod, Monthly satellite-derived phytoplankton pigment distribution for the North Atlantic Ocean basin, *Eos Trans. AGU*, *67*, 835-837, 1986.

Gardner, W. D., I. D. Walsh, and M. J. Richardson, Biophysical forcing of particle production and distribution during a spring bloom in the North Atlantic, *Deep Sea Res.*, *40*, 171-195, 1993.

Geernaert, G. L., Bulk parameterization for the wind stress and heat fluxes, in *Surface Waves and Fluxes*, vol. 1 *Current Theory*, edited by G. L. Geernaert, and W. J. Plant, 332 pp.,Kluwer Academic, Norwell, Mass., 1990.

Hill, P. S., Reconciling aggregation theory with observed vertical fluxes following phytoplankton blooms, *J. Geophys. Res.*, *97*, 2295-2308, 1992.

Holligan, P. M., R. D. Pingree, and G. T. Mardell, Oceanic solitons, nutrient pulses and phytoplankton growth, *Nature*, *314*, 348-350, 1985.

Jerlov, N. G., *Marine Optics*, Elsevier, New York, 1976.

Kiefer, D. A., and D. G. Mitchell, A simple steady-state description of phytoplankton growth based on absorption cross section and quantum efficiency, *Limnol. Oceanogr.*, *28*, 770-776, 1983.

Kirk, J. T. O., *Light and Photosynthesis in Aquatic Ecosystems*, Cambridge University Press, New York, 1983.

Kondo, J., Y. Sasano, and T. Ishii, On wind driven current and temperature profiles with diurnal period in the oceanic planetary boundary layer, *J. Phys. Oceanogr.*, *9*, 360-72, 1979.

Lande, R., and A. M. Wood, Suspension times of particles in the upper ocean, *Deep Sea Res.*, *34*, 61-72, 1987.

Langdon C., J. Marra, and C. Knudson, Measurements of net and gross O_2 production, dark O_2 respiration, and ^{14}C assimilation at the Marine Light-Mixed Layers site ($59°N$, $21°W$) in the northeast Atlantic Ocean, *J. Geophys. Res.*, this issue.

Large, W. G., and S. Pond, Sensible and latent heat flux measurements over the ocean, *J. Phys. Oceanogr.*, *12*, 464-482, 1982.

Marra, J., and C. Langdon, An evaluation of an in situ fluorometer for estimation of chlorophyll *a*, *Tech. Rep. LDEO-93-1*, 36pp, Lamont-Doherty Earth Observ., Palisades, New York, 1993.

Marra J., C. Langdon, and C. A. Knudson, Primary production, water column changes, and the demise of a *Phaeocystis* bloom at the Marine Light-Mixed Layers site ($59°N$, $21°W$) in the northeast Atlantic Ocean, *J. Geophys. Res.*, this issue.

Mellor, G. L. and T. Yamada, Development of a turbulence closure model for geophysical fluid problems, *Rev. Geophys.*, *20*, 851-875, 1982.

Morel, A. and L. Prieur, Analysis of variations in ocean color, *Limnol. Oceanogr.*, *22*, 709-722, 1977.

Nelson, D. M., and W. O. Smith Jr., Sverdrup revisited: Critical depth maximum chlorophyll levels, and the control of Southern Ocean productivity by the irradiance-mixing regime, *Limnol. Oceanogr.*, *36*, 1650-1661, 1991.

Plueddemann, A. J., R.A. Weller, M. Stramska, T. D. Dickey, and J. Marra, Vertical structure of the upper ocean during the Marine Light-Mixed Layers experiment, *J. Geophys. Res.*, this issue.

Plueddemann, A., R. Weller, T. Dickey, J. Marra, G. Tupper, B. Way, W. Ostrom, P. Bouchard, A. Oien, and N. Galbraith, The Marine Light-Mixed Layer Experiment cruise and data report, *Tech. Rep. WHOI-93-33*, 116 pp.,Woods Hole Oceanogr. Inst. Woods Hole, Mass., 1993.

Price, J. F., R. A. Weller, and R. Pinkel, Diurnal cycling: Observations and models of the upper ocean response to diurnal heating, cooling, and wind mixing, *J. Geophys. Res. 91*, 8411-8427, 1986.

Smetacek,V., and U. Passow, Spring initiation and Sverdrup's critical-depth model, *Limnol. Oceanogr.*, *35*, 228-234, 1990.

Smith, R. C. and K. S. Baker, The bio-optical state of ocean waters and remote sensing, *Limnol. Oceanogr.*, *23*, 247-259, 1978.

Smith, R. C., and K. S. Baker, Analysis of ocean optical data, II, *Proc. SPIE Int. Soc. Photo-Opt. Eng.*, *637*, 95-107, 1986.

Spinrad, R. W., H. Glover, B. W. Ward, L. A. Codispoti, and G. Kullenberg, Suspended particle and bacterial maxima in Peruvian coastal waters during a cold water anomaly, *Deep Sea Res.*, *36*, 715-733, 1989.

Stramska, M., and T. D. Dickey, Short-term variations of the bio-optical properties of the ocean in response to cloud-induced irradiance fluctuations, *J. Geophys. Res.*, *97*, 5713-5721, 1992a.

Stramska, M., and T. D. Dickey, Variability of bio-optical properties of the upper ocean associated with diel cycles in phytoplankton population, *J. Geophys. Res.*, *97*, 17,873-17,887, 1992b.

Stramska, M., and T. D. Dickey, Phytoplankton bloom and the vertical thermal structure of the upper ocean, *J. Mar. Res.*, *51*, 819-842, 1993.

Stramska, M., and T. D. Dickey, Modeling phytoplankton dynamics in the northeast Atlantic during the initiation of the spring bloom, *J. Geophys. Res.*, *99*,10,241-10,253, 1994.

Sverdrup, H. U., On conditions of the vernal blooming of phytoplankton, *J. Cons. Int. Explor. Mer*, 18, 287-295, 1953.

Taylor, A. H., and J. A. Stephens, Diurnal variations of convective mixing and the spring bloom of phytoplankton, *Deep Sea Res.* II, 40, 115-134, 1993.

Weller, R. A., and R. E. Davis, A vector measuring current meter, *Deep Sea Res.*, 27, 565-582, 1980.

Wiggert, J., T. Dickey, and T. Granata, The effect of temporal undersampling on primary production estimates, *J. Geophys. Res.*, *99*, 3361-3371, 1994.

Williams, R., Sampling at ocean weather station India, *Ann. Biol. Copenhagen, 32*, 62-64, 1975.

Woods, J. D. and W. Barkmann, The response of the upper ocean to solar heating, I. The mixed layer, *Q. J. R. Meteorol. Soc., 112*, 1-27, 1986.

Woods, J. D., and R. Onken, Diurnal variation and primary production in the ocean- Preliminary results of a Lagrangian ensemble model, *J. Plankton Res., 4*, 735-756, 1982.

T. D. Dickey and M. Stramska, Ocean Physics Group, Department of Earth Sciences, University of Southern California, Los Angeles, CA 90089-0740. (e-mail: stramska@usc.edu; dickey@usc.edu)

C. Langdon and J. Marra, Lamont- Doherty Earth Observatory, Palisades, New York 10964.

A. Plueddemann and R. Weller, Woods Hole Oceanographic Institution, Woods Hole, Massachusetts 08543.